

Computational Measurement of Steric Effects: the Size of Organic Substituents Computed by Ligand Repulsive Energies

David P. White,^{*1} Jan C. Anthony,² and Ademola O. Oyefeso²

Department of Chemistry, University of North Carolina–Wilmington, 601 South College Rd., Wilmington, North Carolina 28403-3297

Received December 8, 1998

Ligand repulsive energies, E_R , have been demonstrated to provide reliable steric parameters for ligands in organometallic systems. E_R values have now been computed for 167 different organic substituents. Three different fragments were employed for the calculation of the ligand repulsive energies: CH_3 , CH_2COOH , and $\text{Cr}(\text{CO})_5$. All compounds were modeled using molecular mechanics. Two different force fields were employed: Allinger's MMP2 and Rappé's Universal Force Field (UFF). Both molecular dynamics and stochastic mechanics were used to determine the lowest energy conformer for each species. Steric sizes were compared against standard steric measures in organic chemistry: Taft–Dubois steric parameter, E_S , A -values, cone angles, θ , and solid angles, Ω_S . Good correlations between E_R and the model-based steric measures (θ and Ω_S) were found. Experimental-based measures, E_S and A -values, showed a mix of steric and electronic effects. On the basis of these correlations, the use of CH_3 , CH_2COOH , and $\text{Cr}(\text{CO})_5$ fragments for steric size quantification was critically examined.

Introduction

Over 100 years ago the importance of the size of a substituent in determining the rate of a given transformation was recognized.³ Sixteen years later the term *steric effect* was coined,⁴ but it took another six years before the first *quantitative measure* of steric effects appeared.⁵ Taft defined a steric parameter, E_S , as the average relative rate of acid-catalyzed ester hydrolysis:⁶

$$E_S = \log\left(\frac{k}{k_0}\right) \quad (1)$$

where k is the observed rate for the acid-catalyzed ester hydrolysis and k_0 is the rate of methyl ester hydrolysis. Values of E_S were averaged over four kinetic measurements: (i) hydrolysis of ethyl esters in 70% aqueous acetone at 25 °C, (ii) hydrolysis of ethyl esters in 60% aqueous acetone at 25 °C, (iii) esterification of carboxylic acids with methanol at 25 °C, and (iv) esterification of carboxylic acids with ethanol at 25 °C. Soon after its definition, it became clear that E_S contained resonance effects. A number of important corrections were made to the defining equation,⁷ but in 1978 Dubois made a major methodological change to Taft's measure.⁸

Dubois accepted the fundamental nature of Taft's measure, but rejected the notion that all four reactions

outlined above would respond identically to steric effects. Therefore, Dubois chose a single standard: the acid-catalyzed esterification of carboxylic acids in methanol at 40 °C. The Taft–Dubois steric parameter, E_S , has become one of the standard measures of steric effects in organic chemistry.⁹

In 1955 Winstein and Holness introduced the concept of an A -value.¹⁰ A -values are free energy differences between axial and equatorial isomers of monosubstituted cyclohexanes:

$$A\text{-value} = -\Delta G^\circ = \frac{RT \ln K}{1000} \quad (2)$$

If the A -value is positive, the equatorial isomer is favored over the axial. Since its inception, a number of important lists of A -values have appeared.^{11,12}

Quantification of steric effects in organometallic chemistry took a very different path. In 1970 Tolman defined

(8) (a) Lomas, J. S.; Luong, P. K.; Dubois, J.-E. *J. Am. Chem. Soc.* **1977**, *99*, 5478. (b) MacPhee, J. A.; Panaye, A.; Dubois, J.-E. *Tetrahedron Lett.* **1978**, 3293. (c) Panaye, A.; MacPhee, J. A.; Dubois, J.-E. *Tetrahedron Lett.* **1978**, 3297. (d) Dubois, J.-E.; MacPhee, J. A.; Panaye, A. *Tetrahedron Lett.* **1978**, 4099. (e) Lomas, J. S.; Dubois, J.-E. *Tetrahedron* **1978**, *34*, 1597. (f) MacPhee, J. A.; Panaye, A.; Dubois, J.-E. *Tetrahedron* **1978**, *34*, 3553. (g) MacPhee, J. A.; Panaye, A.; Dubois, J.-E.; LeRoy, F.; Hospital, M. *Tetrahedron Lett.* **1979**, 653. (h) Lion, C.; Dubois, J.-E.; MacPhee, J. A.; Bonzougou, Y. *Tetrahedron* **1979**, *35*, 2077. (i) Panaye, A.; MacPhee, J. A.; Dubois, J.-E. *Tetrahedron Lett.* **1980**, *21*, 3485. (j) Panaye, A.; MacPhee, J. A.; Dubois, J.-E. *Tetrahedron* **1980**, *36*, 759. (k) MacPhee, J. A.; Dubois, J.-E. *Tetrahedron* **1980**, *36*, 775. (l) MacPhee, J. A.; Panaye, A.; Dubois, J.-E. *J. Org. Chem.* **1980**, *45*, 1164.

(9) See, for example, (a) Isaacs, N. *Physical Organic Chemistry*, 2nd ed.; Longman: Essex, England, 1995; Chapter 8. (b) Dubois, J.-E.; Mouvier, G. *Tetrahedron Lett.* **1963**, 1325. (c) Clark, J.; Perrin, D. D. *Quart. Rev.* **1964**, *18*, 295. (d) Barlin, G. B.; Perrin, D. D. *Quart. Rev.* **1966**, *20*, 75. (e) Pearce, P. J.; Simkins, R. J. *J. Can. J. Chem.* **1968**, *46*, 241. (f) Fellous, R.; Luft, R. *Tetrahedron Lett.* **1970**, 1505. (g) Gallo, R.; Channon, M.; Lund, H.; Metzger, J. *Tetrahedron Lett.* **1972**, 3857. (h) Berg, U.; Gallo, R.; Metzger, J.; Channon, M. *J. Am. Chem. Soc.* **1976**, *98*, 1260. (i) Berndt, D. C.; Ward, I. E. *J. Org. Chem.* **1978**, *43*, 13. (j) Wiberg, K. B.; Squires, R. R. *J. Am. Chem. Soc.* **1979**, *101*, 5512. (k) Neuvonen, K.; Pihlaja, K. *Struct. Chem.* **1995**, *6*, 77.

(1) Email address: whitedp@uncwil.edu.

(2) Undergraduate students from the State University of New York at New Paltz.

(3) Hofmann, A. W. *Chem. Ber.* **1872**, *5*, 704.

(4) Kehrman, F. *Chem. Ber.* **1888**, *21*, 3315.

(5) (a) Meyer, V. *Chem. Ber.* **1894**, *27*, 510. (b) Wegscheider, R. *Monat. Chem.* **1895**, *16*, 75.

(6) Taft, R. W. In *Steric Effects in Organic Chemistry*; Newman, M. S., Ed.; Wiley: New York, 1956; p 556.

(7) (a) Hancock, C. K.; Meyers, E. A.; Yagar, B. J. *J. Am. Chem. Soc.* **1961**, *83*, 4211. (b) Palm, V. A. *Fundamentals of the Quantitative Theory of Organic Reactions*; Khimlya: Leningrad, 1967; Chapter 10. (c) Charton, M. *J. Am. Chem. Soc.* **1969**, *91*, 615. (d) Charton, M. *J. Am. Chem. Soc.* **1969**, *91*, 619. (e) Bellon, L.; Taft, R. W.; Abboud, J.-L. M. *J. Org. Chem.* **1980**, *45*, 1166.

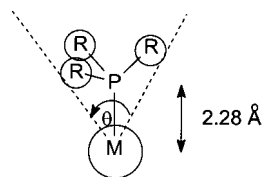


Figure 1. Measurement of the Tolman cone angle for an idealized PR_3 ligand. The $\text{M}-\text{P}$ distance is 2.28 Å, typical of a $\text{Ni}-\text{P}$ bond length.

the cone angle to measure the size of important P-donor ligands.¹³ Tolman built a CPK model of the ligand with the P atom placed 2.28 Å from the metal (a typical $\text{Ni}-\text{P}$ bond distance) and measured the internal angle of an enveloping cone using a protractor (Figure 1).

Since its definition, the cone angle concept has been widely used.¹⁴ In the late 1970s the cone angle methodology was extended to include a variety of organic substituents.¹⁵

Cone angles assume free rotation of the substituent. Thus, the cone angle can be thought of as the maximum steric size of a given group. However, if there is a great deal of steric congestion in a molecule, the cone angle may not be a realistic measure of the amount of space occupied by the substituents as two adjacent groups can mesh to relieve steric strain.¹⁶ Therefore, the solid angle was introduced to quantify steric effects in both organic¹⁷ and organometallic chemistry.¹⁸ Solid angles can be thought of as follows: Suppose a substituent is projected onto the inside of a sphere using some meaningful location for the light source. Then the solid angle, measured in steradians, sr, is the area of the projected

shadow. Mathematically, the solid angle, Ω , at a point O of a surface is represented by the integral

$$\Omega = \int_S \frac{\mathbf{r} \cdot d\mathbf{S}}{r^3} \quad (3)$$

where \mathbf{r} is the position vector of an element of the surface with respect to O, and r is the scalar magnitude of \mathbf{r} . If the entire sphere is covered with shadow, then the solid angle is 4π sr. We may define the fractional solid angle, Ω_s , as:

$$\Omega_s = \frac{\Omega}{4\pi} \quad (4)$$

Most often, the fractional solid angle is more intuitively meaningful than the solid angle measured in steradians. Solid angles contain information about the *shape* of a substituent. In broad terms, if the cone angle represents a *maximum* measure of the steric influence of a substituent, the solid angle represents its *minimum*.

Since solid and cone angles are measured from physical models of substituents, these measures are necessarily free of electronic components. However, we cannot be certain that the experimental-based measures of steric size such as E_s and A -values are free of electronic effects.¹⁰ In addition, some molecules are difficult to synthesize and others do not undergo hydrolysis at a conveniently measurable rate, so model-based measures of steric size are needed to support and supplement measures based on experimental data. These model-based measures also represent a quantification of pure steric effects in the absence of electronic effects.

Brown has developed a new molecular mechanics-based quantification of steric size, the ligand repulsive energy.¹⁹ Ligand repulsive energy values are more intuitively appealing than cone or solid angles because they are computed for a substituent in a prototypical environment. This computation in a prototypical environment is in contrast with cone and solid angles, which measure the size of a group outside of the context of its interactions with a specific molecular entity. Ligand repulsive energies, E_R , have been computed for phosphines, phosphites, arsines, S-donors, O-donors, and olefin ligands.²⁰

The ligand repulsive energy, E_R , is defined as the amount of pure steric repulsion between a ligand and the prototypical molecular fragment to which it is bonded (originally $\text{Cr}(\text{CO})_5$ and subsequently extended to $[(\eta^5\text{-C}_5\text{H}_5)\text{Rh}(\text{CO})]$).^{19,20b} Ligand repulsive energies are computed as follows: (i) The complex consists of a group or ligand whose steric size is to be determined and the molecular fragment to which it is bound (e.g., $\text{Cr}(\text{CO})_5$). Using appropriately defined force field parameters,²¹ this complex is built and energy-minimized in the molecular modeling program Cerius²² (ii) The conformational space of the complex is sampled and the lowest energy conformer selected. (iii) The $\text{Cr}-\text{L}$ bond length is calculated (called r_c) and the van der Waals term in the force

- (10) Winstein, S.; Holness, N. *J. Am. Chem. Soc.* **1955**, *77*, 5562.
 (11) (a) Hirsch, J. A. *Topics Stereochem.* **1967**, *1*, 199. (b) Bushweller, C. H. In *Conformational Behavior of Six-Membered Rings*; Juaristi, E., Ed.; VCH: New York, 1995.
 (12) Eliel, E. L.; Wilen, S. H. *Stereochemistry of Organic Compounds*; Wiley: New York, 1994; Chapter 11.
 (13) Tolman, C. A. *J. Am. Chem. Soc.* **1970**, *92*, 2953.
 (14) (a) Tolman, C. A. *Chem. Rev.*, **1977**, *77*, 313. (b) Brown, T. L.; Lee, K. J. *Coord. Chem. Rev.* **1993**, *128*, 89. (c) White, D.; Coville, N. J. *Adv. Organomet. Chem.* **1994**, *36*, 95.
 (15) (a) Yamamoto, Y.; Aoki, K.; Yamazaki, H. *Inorg. Chem.* **1979**, *18*, 1681. (b) Maitlis, P. M. *Chem. Soc. Rev.* **1981**, *1*. (c) Coville, N. J.; Loonat, M.; White, D.; Carlton, L. *Organometallics* **1992**, *11*, 1081. (d) Imyanitov, N. S. *Koord. Khim.* **1985**, *11*, 1041. (e) Imyanitov, N. S. *Koord. Khim.* **1985**, *11*, 1181. (f) Datta, D.; Tomba, S. G. *J. Chem. Res. Synop.* **1987**, 422. (g) Datta, D.; Majumdar, D. *J. Phys. Org. Chem.* **1991**, *4*, 611.
 (16) (a) DeSanto, J. T.; Mosbo, J. A.; Storhoff, B. N.; Bock, P. L.; Bloss, R. E. *Inorg. Chem.* **1980**, *19*, 3086. (b) Chin, M.; Durst, G. L.; Head, S. R.; Bock, P. L.; Mosbo, J. A. *J. Organomet. Chem.* **1994**, *470*, 73. (c) White, D.; Taverner, B. C.; Leach, P. G. L.; Coville, N. J. *J. Organomet. Chem.* **1994**, *478*, 205. (d) Smith, J. M.; White, D. P.; Coville, N. J. *Polyhedron* **1996**, *15*, 4541. (e) Smith, J. M.; White, D. P.; Coville, N. J. *Bull. Chem. Soc. Eth.* **1996**, *10*, 1. (f) Taverner, B. C.; Smith, J. M.; White, D. P.; Neil, N. J. *S. Afr. J. Chem.* **1997**, *50*, 59.
 (17) (a) Komatsuzaki, T.; Sakakibara, K.; Hirota, M. *Tetrahedron Lett.* **1989**, *30*, 3309. (b) Komatsuzaki, T.; Sakakibara, K.; Hirota, M. *Chem. Lett.* **1990**, 1913. (c) Hirota, M.; Sakakibara, K.; Komatsuzaki, K.; Akai, I. *Computers Chem.* **1991**, *15*, 241. (d) Akai, I.; Sakakibara, K.; Hirota, M. *Chem. Lett.* **1992**, 1317. (e) Komatsuzaki, T.; Akai, I.; Sakakibara, K.; Hirota, M. *Tetrahedron* **1992**, *48*, 1539.
 (18) (a) Immirzi, A.; Musco, A. *Inorg. Chim. Acta* **1977**, *25*, L41. (b) Sheeman, J. I.; Viers, J. W.; Schug, J. C.; Stovall, M. D. *J. Am. Chem. Soc.* **1984**, *106*, 143. (c) Chauvin, R.; Kagan, H. B. *Chirality* **1991**, *3*, 242. (d) McClelland, R. A.; Kanagasabapathy, V. M.; Banait, N. S.; Stenzen, S. *J. Am. Chem. Soc.* **1991**, *113*, 1009. (e) White, D.; Taverner, B. C.; Leach, P. G. L.; Coville, N. J. *J. Comput. Chem.* **1993**, *14*, 1042. (f) White, D.; Johnston, P.; Levendis, I. A.; Michael, J. P.; Coville, N. J. *Inorg. Chim. Acta* **1994**, *215*, 139. (g) White, D.; Taverner, B. C.; Leach, P. G. L.; Coville, N. J. *J. Organomet. Chem.* **1994**, *478*, 205. (h) White, D.; Taverner, B. C.; Coville, N. J.; Wade, P. W. *J. Organomet. Chem.* **1995**, *495*, 41. (i) White, D. P.; Leach, P. G. L.; Coville, N. J. *J. Math. Chem.* **1995**, *18*, 99.

- (19) Brown, T. L. *Inorg. Chem.* **1992**, *31*, 1286.
 (20) (a) Choi, M.-G.; Brown, T. L. *Inorg. Chem.* **1993**, *32*, 1548. (b) Choi, M.-G.; Brown, T. L. *Inorg. Chem.* **1993**, *32*, 5603. (c) Choi, M.-G.; White, D.; Brown, T. L. *Inorg. Chem.* **1994**, *33*, 5591. (d) White, D. P.; Brown, T. L. *Inorg. Chem.* **1995**, *34*, 2718.
 (21) (a) Caffery, M. L.; Brown, T. L. *Inorg. Chem.* **1991**, *30*, 3907. (b) Lee, K. J.; Brown, T. L. *Inorg. Chem.* **1992**, *31*, 289.
 (22) Cerius² is a comprehensive molecular modeling package distributed by MSI, San Diego, CA

field changed from the Buckingham potential:

$$E = D_0 \left\{ \left(\frac{6}{\gamma - 6} \right) \exp \left[\gamma \left(1 - \frac{R}{R_0} \right) \right] - \left(\frac{6}{\gamma - 6} \right) \left(\frac{R_0}{R} \right)^6 \right\} \quad (5)$$

(D_0 is the geometric mean of the potential well depths, γ is a scaling factor, R is the interatomic distance, and R_0 is the arithmetic mean of the van der Waals radii) to the pure repulsive potential,

$$E_{\text{vdW,R}} = D_0 \exp \left\{ \left(1 - \frac{R}{R_0} \right) \right\} \quad (6)$$

(iv) The Cr–L bond length is varied with all other molecular variables constrained, and the van der Waals repulsive energy is calculated. A plot is constructed of van der Waals repulsive energy, $E_{\text{vdW,R}}$, versus distance, r . (v) The ligand repulsive energy is defined as

$$E_{\text{R}} = -r_e \left(\frac{\partial E_{\text{vdW,R}}}{\partial r} \right) \quad (7)$$

In the limit of the small changes made to the Cr–L bond distance, the plot of $E_{\text{vdW,R}}$ versus r is linear. So, E_{R} is the slope of the linear plot of $E_{\text{vdW,R}}$ versus r scaled by r_e .

In the original MM papers, Allinger defined a steric energy as the amount of energy required to distort a molecule from an ideal, strain-free geometry.²³ These energies have been used in the analysis of the steric effects in a number of different organic substrates.²⁴ Brown has demonstrated that total molecular mechanics energy is a poor quantitative measure of steric effects in organometallic chemistry.¹⁹ Brown reasoned that the steric effect exerted by a ligand upon its environment is a consequence of *nonbonded interactions*. Further, Brown found it necessary to exclude repulsion within a ligand to obtain a pure measure of the steric influence of the ligand.¹⁹ This means that ligand repulsive energy is a quantitative measure of the *nonbonded repulsion* between the substituent of interest and the molecular environment surrounding that substituent. Consider, for example, a $\text{Cr}(\text{CO})_5\text{L}$ complex: as the Cr–L bond distance is varied, the total nonbonded repulsion within the ligand is held constant. However, the amount of nonbonded repulsion between ligand and $\text{Cr}(\text{CO})_5$ fragment varies, and this repulsion leads to the ligand repulsive energy parameter.

Even though E_{R} has dimensions of energy, it is not a measure of the ground state thermodynamic energy of a molecule. Rather, E_{R} is a *scaled* parametric measure of pure repulsive energy, in contrast to Allinger's definition and Rüchardt's application of strain energy in MM2.^{23,24} In addition, the ligand repulsive energy is computed with a molecular mechanics-minimized structure. This means that all deviations from the ideal structure, for example bond lengthening, bond angle deformations, etc., have been taken into account prior to the computation of E_{R} . Further, we are interested in obtaining the steric influence of the single conformer of a substituent that is dominant in a reaction, so the single conformer upon which E_{R} is based is generated from a search of the entire

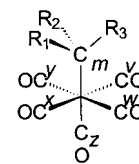


Figure 2. The force field atom labeling scheme used for the molecular modeling of $\text{Cr}(\text{CO})_5\text{R}$ complexes.

conformational space for the substituent in the presence of a prototypical fragment (see below).

The choice of prototypical fragment for the ligand repulsive energy measure needs attention. To allow free rotation about the metal–ligand bond, Brown used prototypical fragments with 2- and 4-fold rotational axes: $[(\eta^5\text{-C}_5\text{H}_5)\text{Rh}(\text{CO})]$ and $\text{Cr}(\text{CO})_5$, respectively.^{19–21} To make a distinction between E_{R} values computed using the original $\text{Cr}(\text{CO})_5$ fragment and ligand repulsive energy values computed using other fragments, we reserve the label E_{R} to refer exclusively to the $\text{Cr}(\text{CO})_5$ fragment. We use $E_{\text{R}}(\text{fragment})$ for ligand repulsive energies computed using all other fragments.

In this paper, we present the application of the ligand repulsive energy methodology to substituents of interest to organic chemists.

Results and Discussion

Choice of Prototypical Fragment. Since organic substituents are generally smaller than the ligands studied by Brown et al., we computed ligand repulsive energies relative to three different fragments: $\text{Cr}(\text{CO})_5$, CH_2COOH , and CH_3 . We retain the original $\text{Cr}(\text{CO})_5$ fragment so that we have a universal standard of E_{R} values for comparison. We anticipate that the CH_2COOH and CH_3 fragments should give steric measures of organic substituents that are intuitively satisfying.

Molecular Mechanics Modeling of the $\text{Cr}(\text{CO})_5\text{R}$, RCH_2COOH , and RCH_3 Species. Unless otherwise noted, a modified MMP2²⁵ force field was used in all calculations. All parameters for the $\text{Cr}(\text{CO})_5\text{R}$ species were obtained from the literature or derived by methods described previously.^{19–21} In the $\text{Cr}(\text{CO})_5$ fragment, the carbonyl groups are either at 180° or 90° from each other. Since we cannot assign two different equilibrium angles to the same interaction, we label each of the five carbonyl C atoms uniquely. Also, we label the donor carbon atom C_m in order to distinguish it from the other carbon atoms in the substituent (Figure 2). All the force field parameters appropriate for an sp^3 -hybridized C atom are used for the newly labeled C_m atom.

Similarly, the carbon atoms between substituent and ipso C atom in the compounds with CH_2COOH or CH_3 fragments are given unique force field labels.

Conformational Searching. The quest to find low energy structures is a central theme in molecular mechanics.²⁶ In general, there are three accepted methods for obtaining a low energy structure: grid search (useful only when there are a moderate number of conformational degrees of freedom in the molecule), stochastic search, or molecular dynamics. Molecular dynamics is the most time efficient of the three methods. In this paper

(23) Burkert, U.; Allinger, N. L. *Molecular Mechanics*; ACS Monograph 177, American Chemical Society: Washington, D. C., 1982

(24) Rüchardt, C.; Beckhaus, H.-D. *Angew. Chem., Int. Ed. Engl.* **1985**, *24*, 529.

(25) (a) Sprague, J. T.; Tai, J. C.; Yuh, Y.; Allinger, N. L. *J. Comput. Chem.* **1987**, *8*, 581. (b) Allinger, N. L. *J. Am. Chem. Soc.* **1977**, *99*, 8127. (c) Allinger, N. L.; Zhou, X.; Bergsma, J. *J. Mol. Struct. (THEOCHEM)* **1994**, *312*, 69.

we use either Monte Carlo stochastic mechanics, molecular dynamics, or a combination of both methods to find the lowest energy structure.

For the $\text{Cr}(\text{CO})_5\text{R}$ complexes, we use a combination of stochastic mechanics and molecular dynamics to find the lowest energy conformation. The structure is built in Cerius² 3.0 or 3.5 and energy-minimized (conjugate gradient minimizer, 500 steps of minimization). This resulting structure is subjected to a Monte Carlo conformation search in which all conformational degrees of freedom are allowed to vary simultaneously by randomly different amounts. Usually, the Monte Carlo search generates 2000 structures, and the lowest energy structure was selected and subjected to molecular dynamics (3.6 ps of molecular dynamics at 500–600 K) and full energy-minimization (SMART minimizer,²⁷ 5000 steps, termination criterion of $0.0100 \text{ kcal mol}^{-1} \text{ \AA}^{-1}$) to ensure a refined minimum energy structure. This final structure was used to determine the ligand repulsive energy.

For the RCH_2COOH structures, the structure was first subjected to several iterations of 0.5 ps of molecular dynamics at 1000 K followed by energy-minimization using the SMART minimizer. The lowest energy structure found by the molecular dynamics methodology was saved and used as the seed structure for stochastic mechanics. Again, 2000 structures were generated in a random conformational search, and the lowest energy structure saved (each structure was subjected to 5000 steps of energy minimization using the SMART minimizer with tight termination criteria of $0.0100 \text{ kcal mol}^{-1} \text{ \AA}^{-1}$). Examining the structures revealed that all of the low energy structures had the same conformation of the CH_2COOH fragment. The CH_3R structures were generated in a manner analogous to the RCH_2COOH structures.

Calculation of Ligand Repulsive Energies. To remain consistent with Brown, we reserve the E_{R} label for the $\text{Cr}(\text{CO})_5$ fragment. Ligand repulsive energies computed relative to the other fragments are called $E_{\text{R}}(\text{CH}_2\text{COOH})$ and $E_{\text{R}}(\text{CH}_3)$. We used a customized code, ERCODE, to calculate ligand repulsive energies.²⁸ Ligand repulsive energy data are presented in Table 1.

To be an acceptable measure of steric size, ligand repulsive energies must make intuitive sense and correlate well with experimental data. As we move across the series Me, Et, *i*-Pr, and *t*-Bu, we find that there is a linear increase in ligand repulsive energy for all fragments (Table 1). Even though experimental evidence indicates that there is an increasing energy penalty with increased substitution,²⁴ the ligand repulsive energy

parameter is based on an isolated component of the total molecular mechanics energy (eqs 6 and 7). This results in a linear trend in E_{R} , which is consistent with cone and solid angle data (which increase by a constant amount, as H atoms in CH_3 are substituted by methyl groups to give *tert*-butyl: for example, $\Omega_{\text{S}}(\text{CH}_3) = 0.206$ (Me), 0.256 (Et), 0.304 (*i*-Pr), and 0.352 (*t*-Bu); see Table 1). As the substituent gets larger, the Taft–Dubois steric parameter gets larger by an increasing amount ($-E_{\text{S}} = 0$ (Me), 0.08 (Et), 0.48 (*i*-Pr), and 1.43 (*t*-Bu); Table 1). Ligand repulsive energies show an intermediate trend dependent upon fragment. The $E_{\text{R}}(\text{CH}_2\text{COOH})$ values show the same trend in increasing ligand repulsive energy as the Taft–Dubois steric parameter: $E_{\text{R}}(\text{CH}_2\text{COOH})$ (in kcal mol^{-1}) = 29 (Me), 37 (Et), 49 (*i*-Pr), and 64 (*t*-Bu); Table 1. With the methyl fragment, $E_{\text{R}}(\text{CH}_3)$ shows a constant increase of 7 kcal mol^{-1} moving from Me to *t*-Bu, similar to the cone and solid angles. Finally, the E_{R} values (with the $\text{Cr}(\text{CO})_5$ fragment) show a trend intermediate between those for $E_{\text{R}}(\text{CH}_2\text{COOH})$ and $E_{\text{R}}(\text{CH}_3)$ (E_{R} (in kcal mol^{-1}) = 17 (Me), 34 (Et), 57 (*i*-Pr), and 60 (*t*-Bu); Table 1).²⁹

Ligand repulsive energy increases for a given fragment with the size of the substituent. However, looking at the data for the series Me, Et, *i*-Pr, and *t*-Bu, we find that the CH_2COOH fragment appears larger than $\text{Cr}(\text{CO})_5$, which is larger than CH_3 : for example for *t*-Bu $E_{\text{R}}(\text{CH}_2\text{COOH}) = 64 \text{ kcal mol}^{-1}$, $E_{\text{R}} = 60 \text{ kcal mol}^{-1}$, $E_{\text{R}}(\text{CH}_3) = 43 \text{ kcal mol}^{-1}$. As the fragment gets smaller, for example the CH_3 fragment, the ligand repulsive energy measure becomes more like the abstract model-based measures of steric size. Using the CH_2COOH fragment, which most closely resembles the ester used for hydrolysis in the measurements of E_{S} , the calculated ligand repulsive energies better match the experimental trend in steric size than for E_{R} or $E_{\text{R}}(\text{CH}_3)$. However, E_{R} values may be more a more generally useful measure of steric requirement, because they are less dependent on specific shape effects than $E_{\text{R}}(\text{CH}_2\text{COOH})$ values.

A second interesting series of data includes the halogens. For example, when we consider CH_3 , CH_2F , CHF_2 , and CF_3 , we find that all the substituents have more or less the same ligand repulsive energies even though the van der Waals radius of hydrogen is about 0.35 \AA smaller than the van der Waals radius of F.³⁰ It appears that the increase in C–F bond length over the C–H bond length compensates for the decreasing van der Waals radius on moving from F to H. Therefore, the CH_3 , CH_2F , CHF_2 , and $-\text{CF}_3$ substituents have approximately the same ligand repulsive energies (Table 1). As further evidence of this trend, we find that the ligand repulsive energies for CH_2X substituents, X = halogen, are more or less constant (Table 1). Only when we consider the CX_3 series, X = H, F, Cl, Br, do we see an increase in ligand repulsive energy as a function of increase in the size of the halogen.³⁰ This suggests that when we have three halogens attached to a single carbon atom, the lengthening of the C–X bond is no longer sufficient to eliminate steric strain at the fragment side of the molecule, and the ligand repulsive energy can increase dramatically.

(26) See, for example, (a) Leach, A. R. In *Reviews in Computational Chemistry*; Kipkowitz, K. B., Boyd, D. B., Eds.; VCH Publishers: New York, 1991; Vol. II, p 1. (b) Li, Z.; Scheraga, H. *Proc. Natl. Acad. Sci.* **1987**, *84*, 6611. (c) Vasquez, M.; Meirovitch, H.; Meirovitch, M. *J. Phys. Chem.* **1994**, *98*, 9380. (d) Meirovitch, H.; Meirovitch, M. *J. Comput. Chem.* **1997**, *18*, 240. (e) McDonald, D. Q.; Still, W. C. *J. Am. Chem. Soc.* **1994**, *116*, 11550. (f) Chang, G.; Guida, W. C.; Still, W. C. *J. Am. Chem. Soc.* **1989**, *111*, 4379. (g) Guarnieri, F.; Still, W. C. *J. Comput. Chem.* **1994**, *15*, 1302. (h) Senderowitz, H.; Guarnieri, F.; Still, W. C. *J. Am. Chem. Soc.* **1995**, *117*, 8211. (i) Senderowitz, H.; Still, W. C. *J. Phys. Chem. B* **1997**, *101*, 1409.

(27) The SMART minimizer was first available in Cerius² 3.0. This minimizer first uses the steepest descent method to locate the approximate minimum and then switches to an adapted basis Newton–Raphson minimizer (first derivative method) and finally to the accurate truncated Newton method (combination of conjugate gradient and full Newton–Raphson second derivatives) to discard saddle points.

(28) Bubel, R. J.; Douglass, T. W.; White, D. P. *J. Comput. Chem.*, submitted. ERCODE automates the calculation of E_{R} with the methodology developed by Brown.

(29) It should be noted that even though there is an increase in 7 kcal/mol for $E_{\text{R}}(\text{CH}_3)$ values upon adding methyl groups, this does not correspond to an increase in strain energy of 7 kcal/mol . Rather, the $E_{\text{R}}(\text{CH}_3)$ increase represents a scaled increase in repulsion between the substituent and methyl fragment.

(30) Bondi, A. *J. Phys. Chem.* **1964**, *68*, 441.

Table 1. Ligand Repulsive Energies (in kcal mol⁻¹), Taft–Dubois Steric Parameters,⁸ Solid Angles, Ω_S ,¹⁷ and Cone Angles, θ (in degrees)^{15f,g} for a Variety of Organic Substituents

substituent	E_R	$E_R(\text{CH}_3)$	$E_R(\text{CH}_2\text{COOH})$	$-E_S^8$	$\Omega_S(\text{CH}_3)^{17}$	$\Omega_S(\text{CO}_2\text{H})^{17}$	$\theta^{15f,g}$
CH ₃	17	20	29	0	0.206	0.211	112
CH ₂ F	20	20	29	0.2	0.228		119
CHF ₂	20	19	29	0.32	0.248		127
CF ₃	21	17	28	0.78	0.268		135
CH ₂ CN	24		31	0.89			
CH ₂ Cl	26	22	33	0.58	0.275		144
CH ₂ OMe	28				0.240		
CH ₂ Br	28	23	34	0.24	0.242		130
CH ₂ I	30	23	34	0.3	0.245		133
cyclopropyl	32	23	31	1.09			
CH ₂ CH=CH ₂	33	27		0.31			
CH ₂ CH ₃	34	27	37	0.08	0.256	0.259	
CHCl ₂	35	26	39	0.58	0.275		144
CH ₂ CH ₂ CH ₂ F	36	27	38				143
<i>n</i> -propyl	36	27	38	0.31	0.269	0.274	143
<i>n</i> -butyl	36	28	38	0.31	0.269	0.276	143
<i>n</i> -pentyl	36	28	38	0.31	0.27	0.272	143
CH ₂ CH ₂ CH ₂ Ph	36	28	38	0.34			143
CH ₂ CH ₂ CH=CH ₂	36	27	38	0.43			
CH ₂ CH ₂ - <i>i</i> -Bu	37	28	39	0.31			
CH ₂ CH ₂ - <i>i</i> -Pr	38	28	39	0.32			
CH ₂ CH ₂ CN	39	27	38				146
CH ₂ CH ₂ - <i>t</i> -Bu	39	29	40	0.33			
CH ₂ COMe	40				0.267		
CH ₂ CH ₂ OH	40	28	37				
CH ₂ CH ₂ Cl	42	29	38		0.257		139
cyclobutyl	42	28	39	0.03			
CH ₂ Ph	42	29	40	0.39			
CH ₂ CH ₂ Br	44	27	38				142
CH ₂ CH ₂ I	44	27	38				145
isobutyl	44	30	43	0.93	0.298	0.305	
CH ₂ - <i>i</i> -Pr	44		43	0.93			
CCl ₃	44	29	42	1.75	0.318		160
CHBr ₂	45	28	42	0.76	0.28		148
CHMeCl	47	30	43				139
CH ₂ (<i>s</i> -Bu)	47		44	0.97			
CH(OH)Me	48	16	45	-0.08			
(CH ₂) ₄ Ph	49	29	38	0.33			143
CHMeBr	50	31	44				141
CH ₂ (OPh)	51	33	44	0.32			
cyclopentyl	52	31	44	0.41			
CHMeI	53	31					144
CH ₂ (<i>t</i> -Bu)	54		44	1.63	0.331	0.338	
CH ₂ CH ₂ Ph	55	27	38	0.35			
CH(Me)(<i>t</i> -Bu)	55	43	59	3.21	0.383	0.391	
CH(OH)(Et)	57	34	46	0.35			
isopropyl	57	34	49	0.48	0.304	0.306	135
cyclohexyl (chair) ^a	59	35	51	0.69			
<i>tert</i> -Butyl	59	43	64	1.43	0.352	0.354	146
CHPh ₂	59	43	57	1.5			
CH(Et)(Me)	61	37	52	0.449			
CH(Me)(Ph)	66	38	53	0.9			
<i>sec</i> -butyl	67	36	52	1	0.326	0.334	154
CH(Et)(Ph)	68	39	54	1.32			
CBr ₃	68	34	52	2.24	0.323		167
CH(Me)(CH ₂ - <i>t</i> -Bu)	69	39	55	1.81			
CH(Me)(<i>n</i> -Pr)	70	37	55	1.02			154
CH(Me)(<i>n</i> -Bu)	70	37	55	1.06			154
CHMe(<i>i</i> -Pr)	71	40		1.94			
CH(Me)(<i>i</i> -Pr)	71	40	54	1.94			
boat cyclohexane ^b	73	35	70	0.69			
CMeBr ₂	73	36	55	1.92			160
CH(<i>n</i> -Pr) ₂	73	40	58	2.03	0.361	0.384	174
CHEt ₂	74	40	57	2	0.356	0.373	174
CH(<i>n</i> -Bu) ₂	74	39	59	2.08			174
CH(Et)(<i>n</i> -Pr)	75	40	57	2			174
CH(Et)(<i>n</i> -Bu)	76	40	57	2.03			174
CMe ₂ Br	79	39	59	1.77			153
CH(Me)(CH ₂ Ph)	80	39	51	0.44			
CH(Et)(<i>i</i> -Pr)	80	42	60	3.23	0.386	0.401	
CH(<i>i</i> -Bu) ₂	81	39	59	2.38	0.382	0.399	
CH(<i>i</i> -Pr)(<i>t</i> -Bu)	87	50	66	6.53	0.453	0.459	
CH(Et)(<i>t</i> -Bu)	88	46	66	5.21			
CH(<i>i</i> -Pr) ₂	89	45	65	5.01	0.418	0.431	
CEt ₃	94	52	75	5.29	0.429	0.429	205
CMe ₂ Et	95	45	67	2.28	0.378	0.387	
C(Me)(Et)(<i>i</i> -Pr)	95	52	74	5.21			
CH(CH ₂ - <i>t</i> -Bu) ₂	102	46	64	3.06			
CMe ₂ (<i>t</i> -Bu)	104	53	83	5.4	0.434	0.44	
CMe ₂ (CH ₂ - <i>t</i> -Bu)	106	53	66	2.48			
CMe ₂ (<i>i</i> -Pr)	107	48	72	3.54	0.404	0.41	
CMeEt ₂	107	49	69	3.63	0.402	0.414	186
CMe(CH ₂ - <i>t</i> -Bu) ₂	110	51	77				
CMe(<i>i</i> -Pr) ₂	113	55	81	7.38			
CEt ₂ (<i>i</i> -Pr)	114	54	76	6.2	0.459	0.46	
CEtPh ₂	116	58	83	4.55			
CMePh ₂	124	56	79	3.73			201
CPh ₃	131	68	89	4.91			228
CH(<i>t</i> -Bu) ₂	131	54	74	6.97	0.473	0.483	
CEt(<i>i</i> -Pr) ₂	136	79	87	5.208			
CEt ₂ (<i>t</i> -Bu)	136	61	95	7.21	0.491	0.491	
CMe(<i>i</i> -Pr)(<i>t</i> -Bu)	143	56	91	5.208			
CEt(<i>i</i> -Pr)(<i>t</i> -Bu)	158	50	78	6.62			
C(<i>i</i> -Pr) ₃	160	69	94	6.73	0.522	0.515	

^a This contains the fragment in the equatorial position. ^b This structure would not minimize in a pure boat conformation. Therefore, a twisted boat is reported.

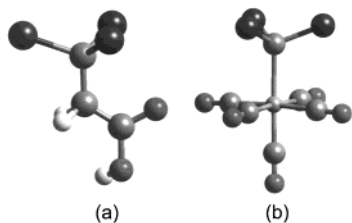


Figure 3. Ball and stick model of (a) $(\text{CBr}_3)\text{CH}_2\text{COOH}$ and (b) $(\text{CBr}_3)\text{Cr}(\text{CO})_5$. Notice how the Br atoms are closer to the basal CO groups in b than they are to the hydrogens and carboxyl group of a. This leads to greater repulsion, and higher ligand repulsion energies, in the $\text{Cr}(\text{CO})_5$ fragment than the CH_2COOH fragment.

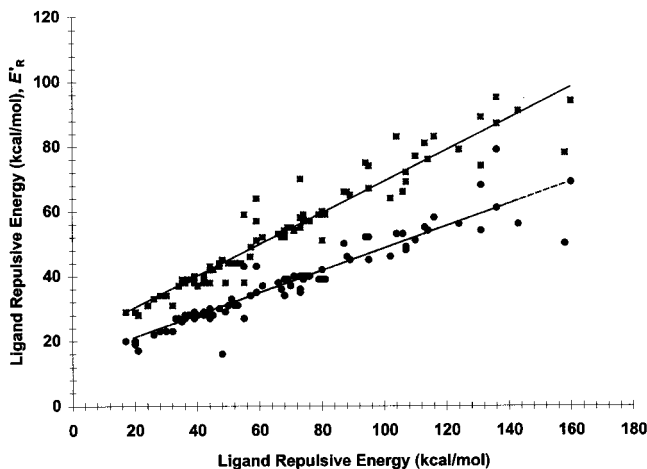


Figure 4. Plot of $E_{\text{R}}(\text{CH}_2\text{COOH})$ and $E_{\text{R}}(\text{CH}_3)$ versus E_{R} for all substituents in Table 1. $E_{\text{R}}(\text{CH}_2\text{COOH})$ data points are shown as gray squares and $E_{\text{R}}(\text{CH}_3)$ as black circles.

For the CBr_3 substituent, we find that the ligand repulsive energy computed against the $\text{Cr}(\text{CO})_5$ fragment is larger than $E_{\text{R}}(\text{CH}_2\text{COOH})$ ($E_{\text{R}} = 68 \text{ kcal mol}^{-1}$, $E_{\text{R}}(\text{CH}_2\text{COOH}) = 52 \text{ kcal mol}^{-1}$; Table 1). The three bromine atoms experience significantly greater repulsion from the basal carbonyl groups that are located in a square plane than from the three substituents in the $\text{CH}_2\text{-COOH}$ fragment that are bent away from the CBr_3 group (Figure 3).

Also, the effective radius of the $\text{Cr}(\text{CO})_5$ fragment is much larger than the effective radius of the CH_2COOH or CH_3 fragments. The effective radius of the fragment is the portion of the fragment that can interact with the substituent. For example, a large substituent will interact sterically with more atoms in $\text{Cr}(\text{CO})_5$ than in CH_3 . The concept of a physical limit to the steric interaction between two ligands has been explored in the literature with $[(\eta^5\text{-C}_5\text{H}_5)(\text{SiMe}_3)_2\text{Fe}(\text{CO})(\text{L})\text{I}]$ complexes, L = phosphine, phosphite, and isonitrile.³¹

To determine which fragment is more sterically congested, we examine the correlation between E_{R} and E_{R}^{20} . There is an excellent correlation between $E_{\text{R}}(\text{CH}_2\text{COOH})$ and E_{R} ($r = 0.962$; slope = 0.485) and $E_{\text{R}}(\text{CH}_3)$ versus E_{R} ($r = 0.939$, slope = 0.343). (See Figure 4.)

Since both slopes are less than one, we can conclude that the size of fragments follow the trend $\text{Cr}(\text{CO})_5 > \text{CH}_2\text{COOH} > \text{CH}_3$ across the whole series of 94 substitu-

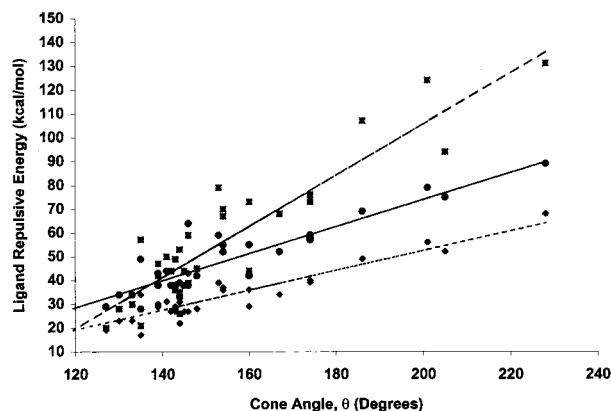


Figure 5. Plot of $E_{\text{R}}(\text{CH}_2\text{COOH})$, $E_{\text{R}}(\text{CH}_3)$, and E_{R} versus cone angle, θ , for all substituents in Table 1. E_{R} data are shown as gray squares, $E_{\text{R}}(\text{CH}_2\text{COOH})$ as black circles, and $E_{\text{R}}(\text{CH}_3)$ as gray diamonds.

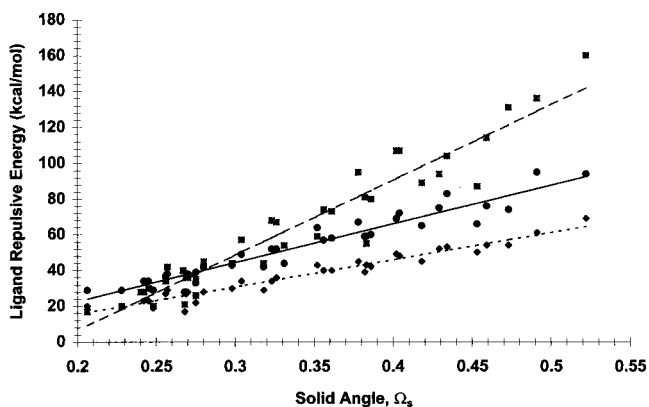


Figure 6. Plot of $E_{\text{R}}(\text{CH}_2\text{COOH})$, $E_{\text{R}}(\text{CH}_3)$, and E_{R} versus Ω_{S} for all substituents in Table 1. E_{R} data are shown as gray squares, $E_{\text{R}}(\text{CH}_2\text{COOH})$ as black circles, and $E_{\text{R}}(\text{CH}_3)$ as gray diamonds.

ents. There is a similarly good correlation between $E_{\text{R}}(\text{CH}_2\text{COOH})$ versus $E_{\text{R}}(\text{CH}_3)$ ($r = 0.957$, slope = 1.31). Since the slope for the plot of $E_{\text{R}}(\text{CH}_2\text{COOH})$ versus $E_{\text{R}}(\text{CH}_3)$ is greater than one, we conclude that the CH_3 fragment is smaller than the CH_2COOH fragment for the 94 substituents examined, as expected. There is somewhat more scatter in the plot of $E_{\text{R}}(\text{CH}_3)$ against E_{R} than in the plot of $E_{\text{R}}(\text{CH}_2\text{COOH})$ against E_{R} . We find that the CH_3 fragment is too small to adequately reflect the steric sizes of large substituents. This is discussed in more detail below.

Our ligand repulsive energy data correlate similarly well with cone¹⁵ and solid angles¹⁷ reported in the literature (Figures 5 and 6).

In all cases, the correlation coefficient is better than 0.9, with the solid angle correlating better with ligand repulsive energies than the cone angle. Cone angles correlate best with $E_{\text{R}}(\text{CH}_3)$ ($r = 0.920$) and worst with $E_{\text{R}}(\text{CH}_2\text{COOH})$ ($r = 0.911$). There are a few outliers in the plots of ligand repulsive energy vs θ . These outliers are either large substituents, for example *t*-Bu and $\text{CMe}_2\text{-Br}$, or contain conformational degrees of freedom, for example $\text{CHMe}(n\text{-Bu})$ and $\text{CHMe}(n\text{-Pr})$ (Figure 5). Since there are no significant outliers in the plots of ligand repulsive energy versus solid angle ($r > 0.959$; Figure 6), we can conclude that the cone angles underestimate the steric size of the large ligands and do not measure the

(31) White, D.; Carlton, L.; Coville, N. J. *J. Organomet. Chem.* **1992**, *440*, 15.

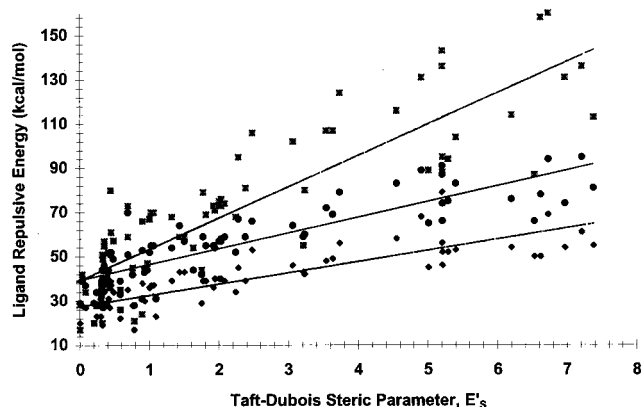


Figure 7. Plot of $E_R(\text{CH}_2\text{COOH})$, $E_R(\text{CH}_3)$, and E_R versus the Taft–Dubois steric parameter, E_S for all substituents in Table 1. E_R data are shown as gray squares, $E_R(\text{CH}_2\text{COOH})$ as black circles, and $E_R(\text{CH}_3)$ as gray diamonds.

conformationally flexible ligands in a conformation realistic to a chemical environment.

We note that the intercepts for the plots of ligand repulsive energy versus θ are nonzero. Brown introduced the concept of an absolute steric threshold, which is the value of θ when ligand repulsive energy is zero.²⁰ The absolute steric threshold represents the onset of steric effects. Absolute steric thresholds for our data are found at $\theta = 84^\circ$ (CH_2COOH fragment), $\theta = 86^\circ$ (CH_3 fragment), and $\theta = 110^\circ$ ($\text{Cr}(\text{CO})_5$ fragment). Similarly, we can derive absolute steric thresholds based on solid angles: For solid angles measured against the CH_3 fragment, $\Omega_S(\text{CH}_3)$, we get steric thresholds at 0.112 (CH_2COOH fragment), 0.110 (CH_3 fragment), and 0.196 ($\text{Cr}(\text{CO})_5$ fragment).

We know that cone and solid angles, by definition, are free of electronic effects.¹⁴ The good correlations between ligand repulsive energy and cone or solid angle indicate that E_R values are also free of electronic terms, as expected. We now turn our attention to correlations between ligand repulsive energy and experimental-based measures of steric effects, E_S ⁸ and A -values.^{10–12} In general there are good correlations between ligand repulsive energies and E_S ($r > 0.85$ in all cases; Figure 7).

It is noteworthy that the outliers are very similar in all plots. Compared to E_S values, ligand repulsive energies are too small for CH_3 , CH_2F , CHF_2 , CF_3 , $\text{CH}_2\text{-CN}$, cyclopropyl, $\text{CH}(i\text{-Pr})(t\text{-Bu})$, and $\text{CMe}(i\text{-Pr})_2$ substituents, irrespective of fragment. It is interesting that of all the halogenated substituents, only the fluorinated series appears as low outliers.

Compared to E_S values, ligand repulsive energies are too large for boat cyclohexyl and $\text{C}(i\text{-Pr})_3$ substituents for all fragments. In addition, certain substituents appear as high outliers in the E_R and $E_R(\text{CH}_3)$ plots (for example, $\text{CEt}(i\text{-Pr})_2$, CMePh_2 , $\text{CMe}(i\text{-Pr})(t\text{-Bu})$, $\text{CEt}(i\text{-Pr})_2$, and CPh_3). Since there are excellent correlations between ligand repulsive energies and cone and solid angles, we may conclude that these data appear as outliers in all comparisons with E_S . Further, the presence of these outliers in the correlations between ligand repulsive energy and E_S suggests that the E_S measure may contain some residual electronic terms.

To clarify whether E_S values contain a residual electronic term, we correlate ligand repulsive energies

with A -values, which are known to contain an electronic component.¹² Unfortunately, the majority of the substituents for which E_S values have been published⁸ (Table 1) do not have available A -values.^{10–12} (We could only find A -values for nine of the substituents listed in Table 1.) In addition, the substituents for which A -values are available are significantly more complicated in structure than the alkyl groups listed in Table 1. We chose to measure ligand repulsive energies for a wide range of substituents for which A -values are available (Table 2) using a slightly modified methodology: the $\text{Cr}(\text{CO})_5$ and CH_2COOH fragments were employed, but the Universal Force Field (UFF)³² was used in place of the MMP2²⁵ force field. (The UFF does not require any additional terms for the bonding of heteroatoms in the $\text{Cr}(\text{CO})_5$ fragment.) Energy-minimized structures were submitted to ERCODE²⁸ for ligand repulsive energy calculation. Correlation between the ligand repulsive energy values generated using the UFF and A -values were poor, with a great deal of scatter (E_R : $r = 0.52$ and $E_R(\text{CH}_2\text{-COOH})$: $r = 0.73$). Ligand repulsive energies are too large for substituents containing polarizable groups such as GePh_3 , OCMe_3 , $\text{Sn}(i\text{-Pr})_3$, CH_2PbMe_3 , and SiCl_3 (Table 2). On the other hand, ligand repulsive energies tend to be too small for linear substituents such as acetylene, $\text{CH}=\text{C}=\text{CH}$, SCN , CN^- , SH , OH , and NH_2 (Table 2). The types of substituents that appear as outliers in the correlation between E_R and E_S also appear as outliers in the plot of ligand repulsive energy (UFF) versus A -values. The similarity in behavior of E_S and A -values in correlations with ligand repulsive energy suggests that the underlying reasons for the scatter are the same. Therefore, we may conclude that both experimental measures of steric size, E_S and A -values, contain some sort of electronic term that is absent in the ligand repulsive energy computation. Brown has noted that a possible origin of this electronic effect is intramolecular dispersion forces between polarizable groups.¹⁹ Given the nature of the experimental-based measures of steric effects, it is inevitable that E_S and A -values contain an implicit measure of polarizability.¹²

Ligand repulsive energies measured with different force fields should be related linearly. To verify this, we took the $\text{RCr}(\text{CO})_5$ complexes for the substituents listed in Table 1, re-minimized them with the universal force field, and recalculated the ligand repulsive energy. We plot E_R^{UFF} (computed with the universal force field) against E_R (computed with the modified MMP2 force field). This allows us to place all the ligand repulsive energies on the same scale. We find the regression equation is

$$E_R = 0.766 E_R^{\text{UFF}} + 2.53 \quad (r = 0.98) \quad (8)$$

indicating that ligand repulsive energy is relatively invariant with respect to force field. Using eq 8, we can recover E_R values for all 167 substituents in this study (Table 3).

Choice of Best Prototypical Fragment for Organic Substituents. The best correlation between ligand repulsive energy and Taft–Dubois steric parameter occurs with $E_R(\text{CH}_2\text{COOH})$ ($r = 0.872$; Figure 7). This is not surprising as E_S is computed using kinetic data from

(32) Rappé, A. K.; Casewit, C. J.; Colwell, K. S.; Goddard, W. A., III; Skiff, W. M. *J. Am. Chem. Soc.* **1992**, *114*, 10024.

Table 2. Ligand Repulsive Energies (in kcal mol⁻¹) Computed Using the Universal Force Field³⁰ and A-Values¹⁰ (in kcal mol⁻¹) for a Variety of Organic Substituents

substituent	$E_{\text{R}}^{\text{UFF}}$	$E_{\text{R}}^{\text{UFF}}(\text{CH}_2\text{COOH})$	A-value	substituent	$E_{\text{R}}^{\text{UFF}}$	$E_{\text{R}}^{\text{UFF}}(\text{CH}_2\text{COOH})$	A-value
HgCl	0.12	1.9	-0.25	CH ₂ Br	36	21	1.79
HgBr	0.13	1.8	0	N=C=NCy	36	16	0.96
HgOAc	0.2	9.4	0	OMe	37	25	0.75
F	0.28	1.8	0.25	OCHO	37	16	0.6
Cl	1	8.1	0.53	OCOCF ₃	37	19	0.68
Br	1.4	6.3	0.48	CH ₂ CH ₃	37	28	1.79
I	2	7.7	0.47	TePh	37	23	0.9
NH ₂	2.8	12	1.23	SiCl ₃	37	30	0.61
CN	2.9	6.6	0.2	OCOCH ₃	38	21	0.87
MgBr	3.3	4.9	0.78	NHMe	38	27	1.29
acetylene	3.7	7.3	0.41	OCONHPh	38	21	0.77
SH	8.1	9.1	1.21	O(<i>p</i> -NO ₂ Ph)	38	20	0.62
OH	9.2	8.1	0.6	OCOPh	38	21	0.5
SiH ₃	10	13	1.45	O(<i>p</i> -anisyl)	39	21	0.7
PH ₂	13	11	1.6	Ph	39	32	2.8
CHO	13	15	0.611	SnMePh ₂	39	28	1.2
SeOPh	14	13	1.25	OPPh ₂	42	35	2.46
COF	17	17	1.4	O(<i>p</i> -ClPh)	42	21	0.65
CH ₃	18	16	1.74	OPh	43	20	0.65
COOMe	19	19	1.2	ONO ₂	44	25	0.62
COOEt	19	19	1.1	SePh	44	15	1
COO ⁻	19	19	2	CF ₃	44	33	2.5
CH=C=CH	19	18	1.53	CH ₂ Ph	46	29	1.68
NO ₂	20	16	1.1	PCl ₂	46	23	1.9
CH=CH ₂	21	21	1.49	SPh	47	18	1.1
CH ₂ HgOAc	22	20	2.05	N=CHCHMe ₂	47	21	0.75
SOMe	23	11	1.2	SnPh ₃	52	29	1.44
SCN	24	13	1.23	CHMe ₂	56	43	2.21
COCl	24	20	1.3	PMe ₂	57	28	1.5
COOH	25	25	1.4	CH ₂ PbMe ₃	58	31	1.81
CH ₂ OH	26	21	1.76	SPPPh ₂	61	35	3.13
SnMe ₂ Ph	26	20	1.08	cyclohexyl	62	52	2.2
CH ₂ OMe	28	23	1.72	CH ₂ SnMe ₃	62	22	1.79
COCH ₃	30	26	1.52	PbMe ₃	62	16	0.67
SMe	31	15	1.04	CH ₂ SiMe ₃	65	27	1.65
CH ₂ CN	31	22	1.77	OCMe ₃	67	37	0.75
SnMe ₃	33	19	1	OSiMe ₃	68	28	0.74
GeMe ₃	34	26	2.1	Sn(<i>i</i> -Pr) ₃	72	36	1.1
POMe ₂	35	22	1.5	GePh ₃	84	41	2.9
NHCOPh	36	26	1.6	PPh ₂	86	35	1.8
SiMe ₃	36	31	2.5	CMe ₃	90	64	4.9

^a This contains the fragment in the equatorial position. ^b This structure would not minimize in a pure boat conformation. Therefore, a twisted boat is reported.

ester hydrolysis.^{6,8} However, we find E_{R} values show the most consistent relative ranking of organic substituent sizes (E_{R} vs E_{S} has $r = 0.869$; Figure 7).

As mentioned above, the CH₃ fragment may be too small to adequately show the repulsion with a large substituent as the substituent can fall outside the effective range of the CH₃ fragment (Figure 8). To understand why the CH₃ fragment is not suitable for ligand repulsive energy measures of organic substituents, consider the -CMe(*i*-Pr)₂ substituent shown in Figure 8 bonded to the CH₃ and Cr(CO)₅ fragments. With the CH₃ fragment (Figure 8a), the isopropyl hydrogens are very close to the hydrogen atoms of the CH₃ fragment. This gives rise to high nonbonded repulsion, according to eq 6. However, as we vary the C_{ipso}-CH₃ bond length to measure the change in van der Waals repulsive energy as a function of distance (eq 7), the van der Waals repulsive energy is more or less constant. This means that the ligand repulsive energy for CMe(*i*-Pr)₂ is too small when computed with the CH₃ fragment and appears as an outlier in Figure 7. On the other hand, with the Cr(CO)₅ fragment (Figure 8b), the molecular mechanics energy-minimized structure shows that the basal carbonyl groups bend away from the CMe(*i*-Pr)₂ substituent. The basal CO groups bend in response to the steric pressure, or van der Waals repulsion, between the isopropyl

hydrogens and the carbonyl groups. This bending is further expressed in an elongation of the equilibrium C_{ipso}-Cr bond length, r_e , which results in a higher E_{R} value (eq 7). Further, as the C_{ipso}-Cr bond distance is adjusted to measure E_{R} , there is a great deal of repulsion between the basal CO groups and the CMe(*i*-Pr)₂ substituent. Both these factors add to give an appropriately large E_{R} value for the CMe(*i*-Pr)₂ substituent.

In general, any substituent that can wrap around the CH₃ fragment (Figure 8a) will show an anomalously low $E_{\text{R}}(\text{CH}_3)$. It is possible that the irregular geometry of the CH₂COOH fragment might also give unexpected results (Figure 3). For example, there should be a preference for a smaller substituent to be syn to the carbonyl group. On the other hand, the Cr(CO)₅ fragment is symmetrical and large enough to show significant repulsion for almost all organic substituents. Therefore, we come to a similar conclusion to that of Brown that the Cr(CO)₅ fragment is robust in its ability to reflect steric sizes of a vast array of different substituents.¹⁹⁻²¹

Conclusions

Steric sizes of 94 substituents have been computed using Brown's ligand repulsive energy methodology. A further 83 ligand repulsive energy values have been

Table 3. Ligand Repulsive Energies (in kcal mol⁻¹) For All Substituents in This Study^a

substituent	E_R	substituent	E_R	substituent	E_R
HgBr	2.6	O(<i>p</i> -anisyl)	32	OSiMe ₃	54
HgCl	2.6	O(<i>p</i> -NO ₂ Ph)	32	CH(Me)(<i>t</i> -Bu)	55
F	2.7	OCONHPh	32	CH ₂ CH ₂ Ph	55
Cl	3.3	OCOPh	32	CH(OH)(Et)	57
Br	3.6	CH ₂ CH=CH ₂	33	isopropyl	57
HgOAc	3.7	Ph	33	Sn(<i>i</i> -Pr) ₃	58
I	4.0	SnMePh ₂	33	CHPh ₂	59
CN	4.7	CH ₂ CH ₃	34	cyclohexyl (chair) ^b	59
NH ₂	4.7	CHCl ₂	35	<i>tert</i> -Butyl	59
MgBr	5.1	O(<i>p</i> -ClPh)	35	CH(Et)(Me)	61
acetylene	5.3	OPh	35	CH(Me)(Ph)	66
SH	8.8	OPPh ₂	35	GePh ₃	67
OH	10	CH ₂ CH ₂ CH=CH ₂	36	<i>sec</i> -Butyl	67
SiH ₃	10	CH ₂ CH ₂ CH ₂ F	36	CBr ₃	68
CHO	13	CH ₂ CH ₂ CH ₂ Ph	36	CH(Et)(Ph)	68
PH ₂	13	<i>n</i> -butyl	36	PPh ₂	68
SeOPh	13	<i>n</i> -pentyl	36	CH(Me)(CH ₂ - <i>t</i> -Bu)	69
COF	16	<i>n</i> -propyl	36	CH(Me)(<i>n</i> -Bu)	70
CH=C=CH	17	ONO ₂	36	CH(Me)(<i>n</i> -Pr)	70
CH ₃	17	SePh	36	CH(Me)(<i>i</i> -Pr)	71
COO ⁻	17	CH ₂ CH ₂ - <i>i</i> -Bu	37	CHMe(<i>i</i> -Pr)	71
COOEt	17	CH ₂ CH ₂ - <i>i</i> -Pr	38	boat cyclohexane ^c	73
COOMe	17	PCl ₂	38	CH(<i>n</i> -Pr) ₂	73
CH=CH ₂	18	CH ₂ CH ₂ CN	39	CMeBr ₂	73
NO ₂	18	CH ₂ CH ₂ - <i>t</i> -Bu	39	CH(<i>n</i> -Bu) ₂	74
CH ₂ F	20	N=CHCHMe ₂	39	CHEt ₂	74
CH ₂ HgOAc	20	SPh	39	CH(Et)(<i>n</i> -Pr)	75
CHF ₂	20	CH ₂ CH ₂ OH	40	CH(Et)(<i>n</i> -Bu)	76
SOMe	20	CH ₂ COMe	40	CMe ₂ Br	79
CF ₃	21	CH ₂ CH ₂ Cl	42	CH(Et)(<i>i</i> -Pr)	80
COCl	21	CH ₂ Ph	42	CH(Me)(CH ₂ Ph)	80
SCN	21	cyclobutyl	42	CH(<i>i</i> -Bu) ₂	81
CH ₂ OH	22	SnPh ₃	42	CH(<i>i</i> -Pr)(<i>t</i> -Bu)	87
COOH	22	CCl ₃	44	CH(Et)(<i>t</i> -Bu)	88
SnMe ₂ Ph	22	CH ₂ CH ₂ Br	44	CH(<i>i</i> -Pr) ₂	89
CH ₂ CN	24	CH ₂ CH ₂ I	44	CEt ₃	94
COCH ₃	25	CH ₂ - <i>i</i> -Pr	44	C(Me)(Et)(<i>i</i> -Pr)	95
CH ₂ Cl	26	isobutyl	44	CMe ₂ Et	95
SMe	26	CHBr ₂	45	CH(CH ₂ - <i>t</i> -Bu) ₂	102
CH ₂ Br	28	CHMe ₂	45	CMe ₂ (<i>t</i> -Bu)	104
CH ₂ OMe	28	PMe ₂	46	CMe ₂ (CH ₂ - <i>t</i> -Bu)	106
SnMe ₃	28	CH ₂ (<i>s</i> -Bu)	47	CMe ₂ (<i>i</i> -Pr)	107
GeMe ₃	29	CH ₂ PbMe ₃	47	CMeEt ₂	107
POMe ₂	29	CHMeCl	47	CMe(CH ₂ - <i>t</i> -Bu) ₂	110
CH ₂ I	30	CH(OH)Me	48	CMe(<i>i</i> -Pr) ₂	113
N=C=NCy	30	(CH ₂) ₄ Ph	49	CEt ₂ (<i>i</i> -Pr)	114
NHCOPh	30	SPPH ₂	49	CEtPh ₂	116
SiMe ₃	30	CH ₂ SnMe ₃	50	CMePh ₂	124
OCHO	31	CHMeBr	50	CH(<i>t</i> -Bu) ₂	131
OCOCF ₃	31	PbMe ₃	50	CPh ₃	131
OCOCH ₃	31	CH ₂ (OPh)	51	CEt(<i>i</i> -Pr) ₂	136
OMe	31	CH ₂ SiMe ₃	52	CEt ₂ (<i>t</i> -Bu)	136
SiCl ₃	31	cyclopentyl	52	CMe(<i>i</i> -Pr)(<i>t</i> -Bu)	143
TePh	31	CHMeI	53	CEt(<i>i</i> -Pr)(<i>t</i> -Bu)	158
cyclopropyl	32	CH ₂ (<i>t</i> -Bu)	54	C(<i>i</i> -Pr) ₃	160
NHMe	32	OCMe ₃	54		

^a E_R^{UFF} values have been corrected using eq 8. ^b This contains the fragment in the equatorial position. ^c This structure would not minimize in a pure boat conformation. Therefore, a twisted boat is reported.

measured using the universal force field,³² and scaled to equivalent E_R values. Molecular mechanics modeling and conformational searching using molecular dynamics and stochastic mechanics on the RCH₃, RCH₂COOH, and RCr(CO)₅ compounds were carried out to yield consistent low-energy conformers. The ligand repulsive energies that were generated showed trends that were intuitively reasonable. Correlations against standard model-based steric measures in organic chemistry were good, but correlations with E_S and A -values suggest that there is an electronic term in the experimental-based measures of steric size. As described by Brown, this electronic term may be of the form of an intramolecular polarizable effect.¹⁹ By using a more general universal force field,

we have demonstrated that ligand repulsive energies can easily be computed for vastly different substituents (Table 3), and the method is sufficiently general to be applied to a large number of molecular fragments of interest in organic and biochemistry. We find that E_R values obtained using the Cr(CO)₅ fragment provide the most consistent and generally useful measures of relative steric sizes.

Methods

All molecular mechanics calculations were performed on a Silicon Graphics Iris Indigo² R10000 or Silicon Graphics O² R10000 workstation using Cerius² 3.0 or Cerius² 3.5 comprehensive molecular modeling software produced by Molecular

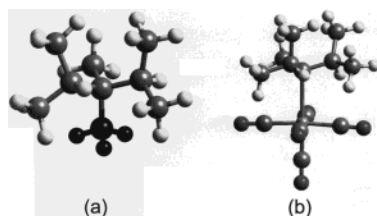


Figure 8. Illustration of the effective steric range of the CH_3 fragment shown for (a) $(\text{CMe}(i\text{-Pr})_2)\text{CH}_3$ and (b) $(\text{CMe}(i\text{-Pr})_2)\text{-Cr}(\text{CO})_5$. In (a) the CH_3 fragment is shown in black. Notice how the methyl groups of the $i\text{-Pr}$ portions of $\text{CMe}(i\text{-Pr})_2$ envelop the CH_3 fragment (a). This leads to constant van der Waals repulsive energy as the C–C bond length is varied to measure E_R (eq 7). The basal CO groups (b) are bent away from the $i\text{-Pr}$ groups to alleviate steric strain in the complex.

Simulations, Inc.²² Either a modified MMP2²⁵ force field, with modifications listed in previous publications dealing with ligand repulsive energy calculations,^{19–21} or an unmodified Universal Force Field³² was employed in the study.

The parameters for the $\text{R-Cr}(\text{CO})_5$ complexes were obtained by analogy with those for the (η^2 -olefin) $-\text{Cr}(\text{CO})_5$ complexes.^{20d} The Cr–C stretching force constant was set at $1.36 \text{ m dyn } \text{\AA}^{-1}$, and strain free distance at 1.79 \AA , as described in the literature.^{20d} We find that minor variation in the Cr–C stretching force constant and equilibrium distance does not affect the relative ordering of ligand repulsive energies.^{20c,d}

Organic compounds, RCH_3 and RCH_2COOH , were modeled using parameters from the literature.²⁵

Energy minimization was carried out using the conjugate gradient minimizer (with termination criteria of $0.100 \text{ kcal mol}^{-1} \text{ \AA}^{-1}$ and a step size of 2.00 \AA) or the SMART minimizer

(with a termination criterion of $0.0100 \text{ kcal mol}^{-1} \text{ \AA}^{-1}$). Monte Carlo conformational searching was carried out by simultaneously varying all rotatable bonds by randomly different amounts to generate 2000 conformers. These conformers were submitted to 18 cycles of anneal dynamics or several cycles of simple dynamics. In the anneal dynamics 18 cycle set, the temperature was ramped from 580 to 600 K in 1 K steps. During each temperature interval, 50 molecular dynamics steps were performed, each lasting 0.001 ps. The final structure was energy minimized with the SMART minimizer and used as the starting structure for the next anneal cycle. Up to three sets of 18 cycles were used to obtain a good representation of the global minimum. Alternatively, the structure was submitted to several iterations of 0.5 ps of simple dynamics at 1000 K followed by energy minimization with the SMART minimizer.

Ligand repulsive energies were calculated using ERCODE,²⁸ implementing the method described by Brown.¹⁹

Acknowledgment. D.P.W. gratefully acknowledges the Beckman Institute for Advanced Science and Technology, University of Illinois at Urbana-Champaign, for summer stipends for 1997 and 1998. Much of the work described in this manuscript was carried out at the State University of New York at New Paltz. We thank Professor Theodore L. Brown, University of Illinois, for valuable discussions, and T. Warthen Douglass, Robert J. Bubel, and Adam Czyski for assistance with data generation. The research was supported by the Research Corporation through the Cottrell College Science Award CC5053.

JO982405W